Journal of Pharmaceutical and Biomedical Analysis Open 3 (2024) 100024

Contents lists available at ScienceDirect

Journal of Pharmaceutical and Biomedical Analysis Open

journal homepage: www.journals.elsevier.com/journal-of-pharmaceutical-and-biomedical-analysis-open

Comparative physicochemical and biological characterization of the similar imiglucerase product Glurazyme® and the originator product Cerezyme®

Maksim Smolov *, Serge Taran, Ivan Lyagoskin, Maria Neronova, Maksim Degterev, Rakhim Shukurov

Joint Stock Company "Generium", Vladimirskaya 14, Volginskiy 601125, Russian Federation

ARTICLE INFO

Keywords:
Imiglucerase
Glurazyme
Cerezyme
Biosimilar
Enzyme replacement therapy (ERT)
Comparative characterization

ABSTRACT

A biosimilar considered as a biomolecule medicinal product that is comparable to a reference medicinal product in terms of the structural, functional, biological, and clinical attributes. Glurazyme® was developed as a biosimilar to Cerezyme® (imiglucerase) and was approved in CIS countries (Russian Federation, Belarus, Kazakhstan) and recently Algeria for the treatment of type 1 and type 3 Gaucher disease. The quality assessment of Glurazyme® was performed in accordance with the Rules for the Study of Biological Medicines of the Eurasian Economic Union harmonized with the ICH comparability guideline and the biosimilar guidelines of the European Medicines Agency and Food and Drug Administration. Extensive side-by-side comparison was employed with state-of-the-art and orthogonal assays designed to interrogate all expected physicochemical and biological activities, including those known to affect the mechanisms of action for imiglucerase. Similarity evaluation was performed on the basis of tolerance intervals determined from about 10 lots of commercial Cerezyme®. Mainly three discrepancies of quality attributes were established concerning oxidized and deamidated forms as well as phosphorylated oligomannose N-glycans reflecting the difference between cultivation and down-stream processes of both medicinal products. Nevertheless, all of them possess a little or no influence on safety and efficacy.

1. Introduction

Gaucher disease is a hereditary autosomal recessive disorder caused by a deficiency of lysosomal enzyme β-glucocerebrosidase (D-glucosyl-N-acylsphingosine glucohydrolase, EC 3.2.1.45) encoded by GBA1 human gene. Since natural substrates of glucocerebrosidase represent N-acyl-sphingosyl-1-O-β-D glucosides with varying fatty acid fragments and sphingosines, a respective disorder is referred to as sphingolipidosis. While active β-glucocerebrosidase promotes the cleavage of glucosylceramide (also called glucocerebroside) into glucose and ceramide, this prevents the accumulation of cellular metabolism products within lysosomes of macrophages [1,2].

Gaucher disease is usually considered as the most common of lysosomal storage disorders and manifests itself in approximately one of 75,000 births worldwide [3,4]. The disease prevalence is the highest among Ashkenazi population (1 per 855 people). In Russia, the averaged incidence is about 1 per 360,000 people that totally corresponds to about 400 patients [5].

Enzyme replacement therapy promotes activation of sphingolipids cleavage and thereby prevents their further accumulation, that is currently considered to be an effective mean against Gaucher disease. The first product based on human placental glucocerebrosidase (alglucerase) was approved by FDA in 1991 for parenteral use under the trade name Ceredase®. In modern practice recombinant glucocerebrosidase analogs: i.e. imiglucerase, velaglucerase alfa, and taliglucerase alfa are the most obvious [6].

Imiglucerase, differing from human placental β-glucocerebrosidase by only one R495H amino acid substitution, was developed and manufactured by Genzyme Corp. under the trade name Cerezyme® since 1994. This medicinal product has been successfully used for chronic treatment in patients with a confirmed diagnosis of type 1 Gaucher disease (without neuropathic manifestations) or type 3 (with chronic neuropathic manifestations) [7,8]. The glycoprotein is produced using a modified CHO cell line transfected with a synthetic gene.

Purified imiglucerase represents monomeric glycoprotein with a molecular mass of approximately 60 kDa. A matured molecule consists of 497 amino acids remaining after N-terminal leader sequence processing. The tertiary structure demonstrates a three-domain

* Corresponding author.
E-mail address: smolov@ibcgenerium.ru (M. Smolov).

https://doi.org/10.1016/j.jpbao.2023.100024
Received 29 September 2023; Received in revised form 1 December 2023; Accepted 11 December 2023
Available online 12 December 2023

organization. The first one (residues 1–27 and 383–414) consists of a three-stranded antiparallel β-sheet flanked on the one side by a perpendicular strand and a looped region on the other. Thus, a pair of N-terminal strands interacts with two antiparallel strands of inner region. Additionally, it contains two disulfide bridges (residues 4–16 and 18–23) necessary to stabilize the whole structure. The catalytic domain (residues 76–381 and 416–430) is formed by a classical triose-phosphate isomerase (TIM) barrel packing $(\beta/\alpha)_8$, that is consistent with an overall A-family glycosylhydrolase homology [9]. Contrasting to the first one this domain contains free cysteine residues at positions 126, 248, and 342. Catalytic domain closely interacts with N-terminal domain forming an active site cavity with one of its loops [10]. As for C-terminal domain (residues 30–75 and 431–497) it is composed of two β-sheets closely packed likewise an immunoglobulin fold and is connected to the catalytic core-domain by a flexible linker (Supplementary Fig. 1s).

Glucocerebroside is an active component of cell membranes; therefore, β-glucocerebrosidase is assumed to be able to interact with a lipid bilayer. The last is evidenced by the observed hydrolysis stimulation in the presence of saposin C binding activator [11]. Also structural studies have revealed the presence of sulfate and phosphate ions bound to the globule, which is consistent with phospholipid composition [12].

Here we describe the results of comparative "state-of-the-art" characterization of two imiglucerase products: the original Cerezyme® used as a reference for the study of a biosimilar Glurazyme® product that has been approved for the market since 2019.

2. Materials and methods

Before the study seven of the methods (Supplementary Table 1s) were validated according to principal recommendations of [13]. The other were qualified as appropriate for the intended purpose on site with a sufficient number of controls.

2.1. Materials

Glurazyme® (Generium LLC., Russia) is formulated with the same active ingredient (1 mg/ml of imiglucerase) and with the same formulation compounds (mannitol, sodium citrate, and polysorbate 80) as Cerezyme® (Genzyme Europe B.V., Netherlands).

LC-MS grade > 99.9% acetonitrile (ACN) was purchased from Merck KGaA (Darmstadt, Germany). Dithiotreitol (DTT), iodoacetic acid, urea, tris(hydroxymethyl)aminomethane (Tris), ethylenediaminetetraacetic acid (EDTA), trifluoroacetic acid (TFA), ammonium formate, perchloric acid, Triton™ X-100, N-ethylmaleimide, 4-nitrophenyl-β-D-glucopyranoside (pNP-G), 4-methylumbelliferyl-β-D-glucopyranoside, sodium phosphate, sodium chloride, bovine serum albumin (BSA), 4-(2-hydroxyethyl)piperazine-1-ethanesulfonic acid (HEPES), Coomassie brilliant blue R-250, sodium dodecyl sulfate (SDS), sodium taurocholate, ammonium acetate, glycine, mannan, magnesium chloride and calcium chloride were purchased from Sigma-Aldrich (Burlington, USA). LC-MS grade > 99.0% formic acid, as well as Ham's F-12 K medium were purchased from Fisher Scientific (Pittsburgh, USA). Hydrochloric acid, citric acid, sodium citrate, sorbitol, potassium phosphate, guanidine and potassium chloride were purchased from PanReac AppliChem (Darmstadt, Germany). Surfactant P20 was purchased from Cytiva (Marlborough, USA). Phosphate buffer saline (PBS) was purchased from PanEco (Moscow, Russia).

Amicon® Ultra-4 10 K ultrafiltration units (Merck Millipore, Burlington, USA) as well as dialysis bags with molecular weight cutoff 10 kDa (Thermo Scientific, Waltham, USA) were used for buffer exchange.

2.2. Peptide mapping

To achieve denaturation a number of 0.5 ml aliquots of imiglucerase (1 mg/ml) solution were mixed with 0.5 ml of denaturing buffer (100 mM Tris-HCl, pH 8.6, 8 M urea, 1 mM EDTA) and incubated at 50 °C for 30 min. Further disulfide bonds were reduced with 10 mM DTT for 1 h at 50 °C, followed by 25 mM iodoacetic acid alkylation for 30 min at 5 °C. Samples were transferred to 0.25 ml of 0.075% TFA by means of Amicon® Ultra-4 10 K ultrafiltration, where 28 μl of hydrolysis buffer (350 mM Tris-HCl, pH 8.5) with 10 μg of trypsin (#V5111, Promega, Madison, USA) were added. The resulting mixtures were incubated at 37 °C for 4 h, then 1 μl of formic acid was added, mixed and centrifuged for 2 min at 13,400 g followed by supernatant analysis by means of Nexera X2 HPLC system equipped with SPD-M30A PDA detector (Shimadzu Corporation, Kyoto, Japan) and Q Exactive HF Biopharma quadrupole-orbital ion trap mass spectrometer (Thermo Scientific, Waltham, USA). An ACQUITY UPLC Peptide CSH C18, 2.1 × 100 mm, 1.7 μm, 130 Å column (Waters, Milford, USA) was used at 45 °C and 0.35 ml/min flowrate along with 0.1% formic acid/acetonitrile gradient (0–2.5 min – 1% ACN; 54 min – 40% ACN; 56–61 min – 98% ACN; 61.1–67 min – 1% ACN). A 210 nm UV absorption signal was recorded while frontal and tandem MS data were collected for each peak. The mass spectrometer was equipped with a HESI II source and operated in a positive ionization $ddMS^2$ mode. The sheath and aux gas flow rates were 25 and 10 units, respectively. The capillary temperature was set at 250 °C, aux gas temp at 350 °C. The spray voltage was set at 3.5 kV. AGC target was set at 1×10^6 in frontal scan mode and 2×10^5 in tandem scan mode. Resolution was set at 120 000 in frontal scan mode and 45 000 in tandem scan mode. The frontal scan m/z range was 200–2 000 Th. Max. inject time was set at 100 ms in frontal scan mode and 80 ms in tandem scan mode. The HCD NCE level was set at 30 units. The resulting data were processed and searched against the sequence of imiglucerase using Peaks AB, v 2.0 software (Bionformatics Solutions Inc., Waterloo, Canada). The experimental date for the site-specific glycan profiling were also evaluated with BYOS (Protein Metrics Inc., Cupertino, USA) software. A fixed modification of alkylated cysteine was specified, and standard modifications typically observed in proteins were set as variable. The relative percent PTMs were calculated as a relative intensity of modified peptide versus the sum of modified and unmodified peptide intensities.

2.3. UV-spectroscopy

Before optical measurements, all samples were dialyzed in the same container against 1 l of the buffer (20 mM sodium phosphate, pH 6.2, 50 mM sodium chloride): 7.5 ml of each stock solution at + 4 °C in dialysis bags with molecular weight cutoff 10 kDa, once for 15 h, three times for 2 h. The dialyzed fractions and buffer used at the last dialysis were measured. Cary 100 spectrophotometer (Varian Inc., Palo Alto, USA) was used in a two-beam absorption scanning mode in 240–350 nm range with 1 nm increment and a 2 nm spectral gap with 0.1 s signal averaging. An extinction coefficient of 1.75 $l \cdot g^{-1} cm^{-1}$ was employed for concentration estimate taking in further measurements.

2.4. FTIR-spectroscopy

Imiglucerase samples were studied with Nicolet 6700 FTIR spectrometer (Thermo Scientific, Waltham, USA) in the transmission mode with crystal CaF_2 cuvette (4 μm optical path) equipped with MCT detector scanning in between 650 cm^{-1} to 4000 cm^{-1} range with 1 cm^{-1} resolution. Before the measurements previously dialyzed samples were concentrated by Amicon® Ultra-4 10 K units to maintain a concentration of around 50 mg/ml. An averaging of 256 repeated spectra was proceeded for each sample.

2.5. Circular dichroism

All far- and near-CD measurements were registered with dialyzed (0.05 or 0.46 mg/ml) samples by J-810 spectropolarimeter (JASCO Inc., Easton, USA). Far-UV region was step-by-step scanned in the range from 200 to 250 nm with 1 nm increment and a 2 nm spectral gap averaging for 2 s while for the near-UV region (250–350 nm) averaging time took 1 s only.

2.6. Intrinsic fluorescence

An aromatic residues fluorescence was measured with dialyzed 0.06 mg/ml samples by Cary Eclipse (Varian Inc., Palo Alto, USA) instrument with 280 nm excitation wave and 5 nm and 2.5 nm spectral gaps for actuating and analyzing monochromators, respectively. The emission spectra were measured from 300 nm to 410 nm wavelength range with 2 nm increment and 1 s data averaging. A detecting PMT voltage was established at 800 V.

2.7. SDS-PAGE

Analysis was performed with 2.5 μg imiglucerase samples denatured by 50 mM DTT in presence of 1% SDS for 5 min at 98 °C. Separation on Mini-PROTEAN® TGX™ Precast Protein 4–20% mini gel (BioRad Laboratories Inc., Hercules, USA) was performed as described by manufacturers' protocol [14].

2.8. Intact mass measurements

The analysis was performed by HPLC Nexera X2 (Shimadzu Corporation, Kyoto, Japan) system equipped with Q Exactive HF Biopharma mass spectrometer (Thermo Scientific, Waltham, USA). An AdvanceBio™ SEC 200 Å, 2.1 × 150 mm, 1.9 μm column (Agilent Technologies, Santa Clara, USA) was used to perform quick separation in 60 μl/min mobile phase (80 mM ammonium acetate) flow at 25 °C. An injecting volume corresponded to 10 μl for 1 mg/ml concentrated samples. The mass spectrometer was equipped with a HESI II source and operated in a positive ionization HMR mode. The sheath and aux gas flow rates were 40 and 30 units, respectively. The spray voltage was set at 3,4 kV. In source CID energy was set at 15 eV. AGC target was set at $1 * 10^6$. Resolution was set at 30 000 with *m/z* range from 2 500–8 000 Th. Max. inject time was set at 100 ms. The experimental data were processed using Biopharma Finder v 3.2 software (Thermo Scientific, Waltham, USA).

2.9. Ellman's assay

Here 10 mg/ml solutions of imiglucerase were prepared in a denaturing buffer (0.1 M Tris-HCl, pH 8.0, 5 M guanidine, 1.7 mM EDTA) with Amicon® Ultra-4 10 K ultrafiltration. A precise concentration was evaluated by measuring 280 nm optical absorbance. To determine the content of thiols, 412 nm optical absorbance was registered after incubation in the presence of 0.34 mM 5,5′-dithio-bis(2-nitrobenzoic acid). When a total thiols amount determined, the samples were preliminary reduced by 10 mM DTT for 1 h at 20 °C followed by its ultrafiltration removal. The content of free 2-nitro-5-thiobenzoate was quantified using the extinction coefficient of 14,150 $M^{-1}cm^{-1}$ in accordance with [15].

2.10. Disulfide bonds mapping

An equal volume of imiglucerase solution (1 mg/ml) was added to 50 μl of denaturing buffer (0.1 M Tris-HCl, pH 7.8, 6 M guanidine, 1 mM EDTA) with further 50 °C incubation for 1 h. The samples were cooled down to RT followed by 14 μl addition of 0.2 M N-ethylmaleimide solution with 4 °C incubation for 1 h. A successive buffer exchange to 0.075% TFA by means of Amicon® Ultra-4 10 K ultrafiltration was performed. At the last cycle the final volume adjusted to 50 μl. Next 10 μl of proteolysis buffer (350 mM Tris-HCl, pH 8.5) and rAsp-N (#V1160, Promega, Madison, USA) solution (0.2 mg/ml) were added to each sample. The samples were mixed and incubated at 37 °C for 6 h. Finally, 5 μl of peptide-N-glycosidase F (#P7367, Sigma-Aldrich, Burlington, USA) solution (0.5 U/ml) was added followed by 37 °C incubation for 18 h. The samples prepared were analyzed on 1290 Infinity II HPLC system connected to 6550 QTOF mass spectrometer (Agilent Technologies, Santa Clara, USA) equipped with ExD fragmentation cell (E-MSIon, Inc., Corvallis, USA). An ACQUITY UPLC Peptide CSH C18, 1.0 × 150 mm, 1.7 μm, 130 Å column (Waters, Milford, USA) was used at 60 °C and 0.08 ml/min flowrate together with 0.1% formic acid/acetonitrile gradient (0–1.5 min – 2%ACN; 58 min – 50% ACN; 62–67 min – 95% ACN; 69–75 min – 2%ACN). The mass spectrometer was equipped with AJS source and operated in a positive ionization autoMS/MS mode for the CID fragmentation and targeted MS/MS mode for the ECD fragmentation. The sheath gas temperature was set at 350 °C with flow rate 12 l/min. The drying gas temperature was set at 200 °C with flow rate 18 l/min. The nebulizer pressure was set at 35 psig. The VCap voltage was set at 2.5 kV with nozzle voltage at 0.9 kV. The frontal scan *m/z* range was 250–2 000 Th, tandem scan range of 50–3 200 Th. The frontal scan rate was 4 Hz, tandem scan rate – 3 Hz for auto MS/MS mode and 0.5 Hz for targeted MS/MS mode. The collision energy for CID fragmentation was set at 20 eV; the filament current for ECD fragmentation was set at 2.49 A. The experimental data were processed using Peaks AB, v 2.0 (Bionformatics Solutions Inc., Waterloo, Canada) and ExD Viewer (E-MSIon, Inc., Corvallis, USA) software.

2.11. Isoelectrofocusing

Isoforms distribution was assessed using a precast polyacrylamide 250 × 110 × 0.5 mm CleanGel (Cytiva, Marlborough, USA) soaked in ampholites mixture (2.5% PL5–8, 3.7% PL 8–10.5, 10% sorbitol). Gel was prefocusing at 0.7 kV for 20 min, when 5 μl of about 2 mg/ml concentrated samples were applied to the anodic side, and then a voltage of 0.5 kV was applied for 20 min. Focusing was performed for 120 min at 2.0 kV, for the last 10 min gel was exposed at 2.5 kV to improve band resolution. Finally, it was fixed with 10% perchloric acid and stained with Coomassie brilliant blue R-250 solution as initially described in [16].

2.12. HILIC

Glycosylation pattern was evaluated by hydrophilic interaction liquid chromatography (HILIC), where oligosaccharides were preliminarily isolated from imiglucerase by treatment with peptide-N-glycosidase F. To increase a sensitivity, the samples were prepared by InstantPC™ GlykoPrep Kit® (#GP96NG-LB, Prozyme, Hayward, USA) following the manufacturers' protocol [17]. HPLC separation was performed with 2.1 × 150 mm, 2.7 μm AdvanceBio Glycan Map column (Agilent Technologies, Santa Clara, USA) by 65 min acetonitrile gradient (75–63%) in 100 mM ammonium formate, pH 4.5, at 0.4 ml/min flowrate and 45 °C. An injecting volume corresponded to 3 μl. The data acquisition was made using Nexera X2 system (Shimadzu Corporation, Kyoto, Japan), equipped with RF-20A xs fluorescence detector capable for 285 nm excitation and 345 nm emission registration. Glycan mass spectra were recorded using a 6550 iFunnel QTOF LC/MS (Agilent Technologies, Santa Clara, USA) mass-spectrometer operated in a high sensitivity mode. The mass-spectrometer was operated with AJS ESI ion source in a positive mode with nozzle voltage set to 0.5 kV, capillary voltage set to 2 kV, and nebulizer pressures set to 33 psig. The sheath gas flowrate was set to 17 l/min (200 °C) while focusing gas flowrate was set to 10 l/min (300 °C). The scanning range was set to 400–2500 *m/z*. MS identification of glycans was performed by Mass Hunter Workstation v 10.0 (Agilent Technologies) software MFE algorithm. For monoisotopic mass calculations a monoisotopic mass additive of IPC-group considered to be as 261.14773 Da.

2.13. Site-specific glycan profiling

Here preparative and analytical protocols were the same as for peptide mapping procedure except mass spectrometry data were processed with a BYOS software (Protein Metrics, Cupertino, USA).

2.14. Size-exclusion HPLC

Alliance e2695 HPLC system equipped with 2475 fluorescence detector were used (Waters, Milford, USA). An AdvanceBio™ SEC 300 Å, 4.6 × 300 mm, 2.7 μm column (Agilent Technologies, Santa Clara, USA) was used to perform separation in 0.3 ml/min mobile phase (49 mM sodium citrate, pH 6.3, 10% acetonitrile) flow at 28 °C. An injecting volume corresponded to 5 μl for 1 mg/ml concentrated samples. A signal of 330 nm fluorescence was recorded when 280 nm excitation was performed.

2.15. Reverse-phase HPLC

Acquity Arc HPLC system equipped with UV/Visible 2489 detector (Waters, Milford, USA) were used. Jupiter C4, 4.6 × 150 mm, 5 μm, 300 Å (Phenomenex Inc., Torrance, USA) column was used to perform separation in 1.0 ml/min mobile phase (0.1% trifluoroacetic acid with acetonitrile) flow at 45 °C. An injecting volume corresponded to 15 μl for 1 mg/ml concentrated samples. Separation was performed in acetonitrile gradient mode: 0–1 min – 35% ACN; 33 min – 65% ACN; 34–39 min – 95% ACN; 40–50 min – 35% ACN. A signal of 214 nm absorbance was collected for the related-impurities estimate. A characterization of fractionized products performed by LC-MS as described for the intact mass measurement section.

2.16. Activity assay

The kinetics of imiglucerase chromogenic 4-nitrophenyl-β-D-glucopyranoside hydrolysis was studied in a 96-well plate. The range of pNP-G substrate working dilution corresponded to 0.15–20 mM prepared in buffer solution (100 mM potassium phosphate, pH 5.9, 20 mM citric acid, 0.125% sodium taurocholate, 0.16% Triton™ X-100 and 0.1% BSA). Each well was placed with 80 μl of corresponding substrate dilution. A plate was pre-warmed to 37 °C temperature prior to the measurements. The reaction was initiated by adding 20 μl of enzyme solution (5 nM final concentration). A 96-well plate was incubating at 37 °C while stop mixture (0.1 M glycine, pH 10.0) 150 μl was introduced after 5, 10, 20, 30, 45, or 60 min followed by an optical density measurement at 405 nm using xMark™ reader (Bio-Rad Laboratories, Inc., Hercules, USA). The substrate conversion rate was evaluated by accumulation of 4-nitrophenol, taking the extinction coefficient equal to 18.3 $mM^{-1}cm^{-1}$. One activity unit (U) defined as the enzyme amount required to convert 1 μmol of the substrate in 1 min at 37 °C.

2.17. SPR study

Surface plasmon resonance (SPR) signal was recorded using the Biacore 8 K system (GE HealthCare, Chicago, USA). Recombinant cation-dependent human macrophage mannose receptor (MMR) CD206 (#CD6-H52H9, Acro Biosystems, Newark, USA) was covalently immobilized on CM5-sensor in accordance with a standard protocol [18]. A specific imiglucerase real time interaction observed in a range from 7 to 200 nM when injecting solutions directly to reference cell (with no receptor) followed by measuring cell containing immobilized MMR. The analysis was performed at 25 °C and 30 μl/min flowrate in duplicates using buffer (0.1 M HEPES, pH 7.4, 1.5 M sodium chloride, 5 mM calcium chloride and 0.5% v/v Surfactant P20). For the association and dissociation time a value of 220 s or 100 s were taken respectively. The resulting sensograms were inspected with Biacore Insight Evaluation Software (GE HealthCare, Chicago, USA), where kinetic dissociation constant (K_D) was determined, resembling the ratio between the decay and association rate for the receptor complex.

2.18. Uptake by macrophages

Peritoneal macrophages obtained from healthy BALB/c mice (~7.5×10^4 cells) were incubated with (150 nM to 10 μM) imiglucerase samples in ham's F-12 K medium and 5% carbon dioxide for 3 h and 37 °C in Galaxy 170 S incubator (New Brunswick Scientific, Cambridge, UK). The cells were then washed twice with ice cold PBS containing 1 mg/ml of mannan additive. To further ensure release of any proteins with its non-specific binding to the membrane one half was washed by ice cold buffer (0.7% glycine-HCl, pH 3.0, 0.8% NaCl, 0.038% KCl, 0.01% $MgCl_2$, and 0.01% $CaCl_2$) followed by two cold PBS washes. The other half was used as control for measuring a total (i.e. bound and internalized) enzymatic activity. A solution of 1% Triton™ X-100 was added to the cells and incubated at 37 °C with stirring for 1 h. Then, the cells were frozen/thawed three times, while the lysis level was monitored with microscope. The resulting lysates were centrifuged with further 20 μl of supernatant transfer to clean 96-well plates. Internalized imiglucerase activity determined by the reaction with 80 μl of 5 mM 4-methylumbelliferyl-β-D-glucopyranoside fluorogenic substrate dissolved in a buffer (100 mM potassium phosphate pH 5.9, 20 mM citric acid, 0.125% sodium taurocholate, 0.16% Triton X-100, 0.1% BSA). Incubation for 30 min at 37 °C performed prior to addition of 150 μl of 0.1 M glycine pH 10.5 solution. The 440 nm fluorescence was measured after 365 nm light excitation with SpectraMax M3 microplate reader (Molecular Devices, San Jose, USA). The fluorescence logarithmic dependence on imiglucerase concentration approximated by a four-parameter sigmoidal plot with successive effective concentration (EC_{50}) estimate. A relative activity was calculated as per cent proportion of test and standard EC_{50} values. A standard value was averaged from Cerezyme® batches statistics.

To assess the internalization specificity incubation of murine peritoneal macrophages was performed in simultaneous presence of both 2.2 μM imiglucerase and 2.5 mg/ml mannan. Fluorescence levels were compared with those for the mixture without mannan.

3. Results

3.1. Structure elements

For the amino acid sequence comparison, a site-specific trypsin proteolysis followed by HPLC-MS peptide separation was performed as a quite sensitive method to discover minor differences between closely related proteins. An example of chromatographic profiles of the original product and similar imiglucerase hydrolysates is shown in Fig. 1. All the peptides peaks of Glurazyme® have its corresponding analogs at Cerezyme® chromatogram, while no unique peaks were detected. By correlating the recorded masses and peptide fragmentation spectra the imiglucerase sequence coverage seemed to be near 100% for both preparations (Supplementary Table 2s).

Peptide mapping allowed for the relative assessment of amino acid modifications via isolated ion current integration (Fig. 2). A 5-fold difference is recorded for the deamidated glutamine 440 content. Three other residues (N192, N333 and Q350) also undergo deamidation but the extent and difference between Glurazyme® and Cerezyme® looks less significant.

The other prevalent modifications are oxidized forms, since ponderable contents of modified amino acids (M123, M450 and some other) is found. Among them no distinct increase or decrease were detected between Glurazyme® and Cerezyme® thus probably reflecting a consequence of a sample preparation procedure rather than real products similarity. Finally, two succinimide containing peptides were registered for N192 and, mainly, for N188 residues equally among the products under the study.

The levels of secondary and tertiary structure organization were evaluated in a comprehensive study using a combination of physicochemical methods, including UV-absorption spectroscopy, circular dichroism, Fourier transform IR spectroscopy, and intrinsic protein fluorescence (Fig. 3 and Supplementary Table 4s).

All the UV spectra has a pronounced maximum near 280 nm due to the presence of aromatic residues, that is consistent with a published

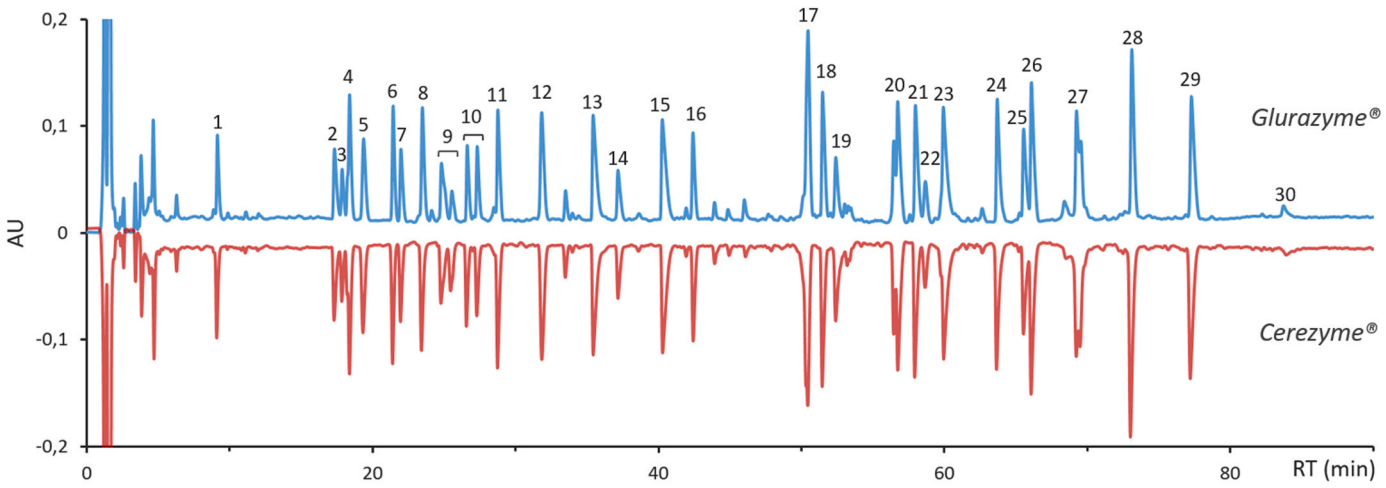

Peak	Peptide	Peak	Peptide	Peak	Peptide	Peak	Peptide	Peak	Peptide
1	322-329;	7	258-262;	13	414-425; 467-473;	19	132-155;	25	164-186;
2	1-7;	8	158-163;	14	278-285;	20	48-74; 396-408;	26	171-186;
3	212-215;	9	263-277; 216-224;	15	286-293;	21	442-463;	27	467-496;
4	434-441; 409-413;	10	180-186; 294-303;	16	121-131;	22	330-346;	28	8-39; 225-257;
5	426-433;	11	347-353;	17	107-120;	23	49-74; 304-321;	29	80-106;
6	164-170; 354-359;	12	199-211;	18	132-157;	24	474-496;	30	360-395;

Fig. 1. Mirror images of UV 210 nm chromatograms of trypsin-generated imiglucerase peptides. Main peaks are enumerated and annotated as amino acid sequences validated with LC-MS/MS.

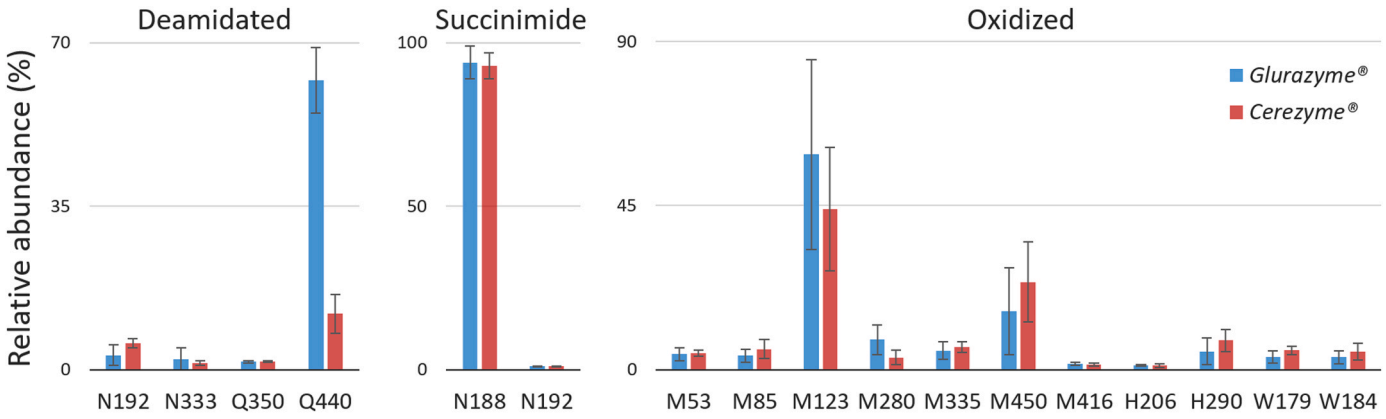

Fig. 2. Summary of imiglucerase % PTMs observed by LC-MS/MS tryptic peptides analysis. The relative abundances were calculated as a relative intensity of modified peptide versus the sum of modified and intact peptides intensities.

data [19]. In addition, the fine spectral structure was also identical for both imiglucerase products (data not shown).

The estimated theoretical content of secondary structure elements is characterized by the predominance of α-helices (28%) and β-sheets (27%), while contribution of disordered areas looks also prevalent (about 40%) [10]. The results obtained from far-UV CD spectra calculations proves a significant contribution of α-helices (about 23%), as well as β-sheets (26–28%) and disordered areas (28–29%), and together with the similarity of near-UV CD spectra account for identical tertiary structures among two imiglucerase products under the study (Fig. 3A and B).

Imiglucerase contains 12 tryptophan and 19 tyrosine residues, allowing intrinsic fluorescence method to be used for the estimate of their local environment. All the fluorescence spectra obtained indicates the predominance of tryptophan contribution while the maximum is located at 334 nm suggesting a moderate residues' exposition to the outer water solvent [20]. Comparison of the fine fluorescence spectra shapes demonstrates no remarkable difference suggesting a similarity of corresponding tryptophan mobilities and polarities (Fig. 3C).

3.2. Molecular mass

When analyzed by slab gel electrophoresis in the presence of SDS the samples of reduced generic and original products were characterized by a single band with 64 kDa mobility (Supplementary Fig. 2s). Taking into account the complex nature of the imiglucerase a high-resolution native mass spectrometry was used to determine the exact molecular masses of major proteoforms. Glurazyme® and Cerezyme® mass spectra demonstrate a formation of ion clusters with a charge distribution from 13 + to 16 + for the imiglucerase monomeric state. The spectra indicate the presence of a number of proteoforms distributed in the range from about 59.5–60.5 kDa consistently to published data [12]. As imiglucerase

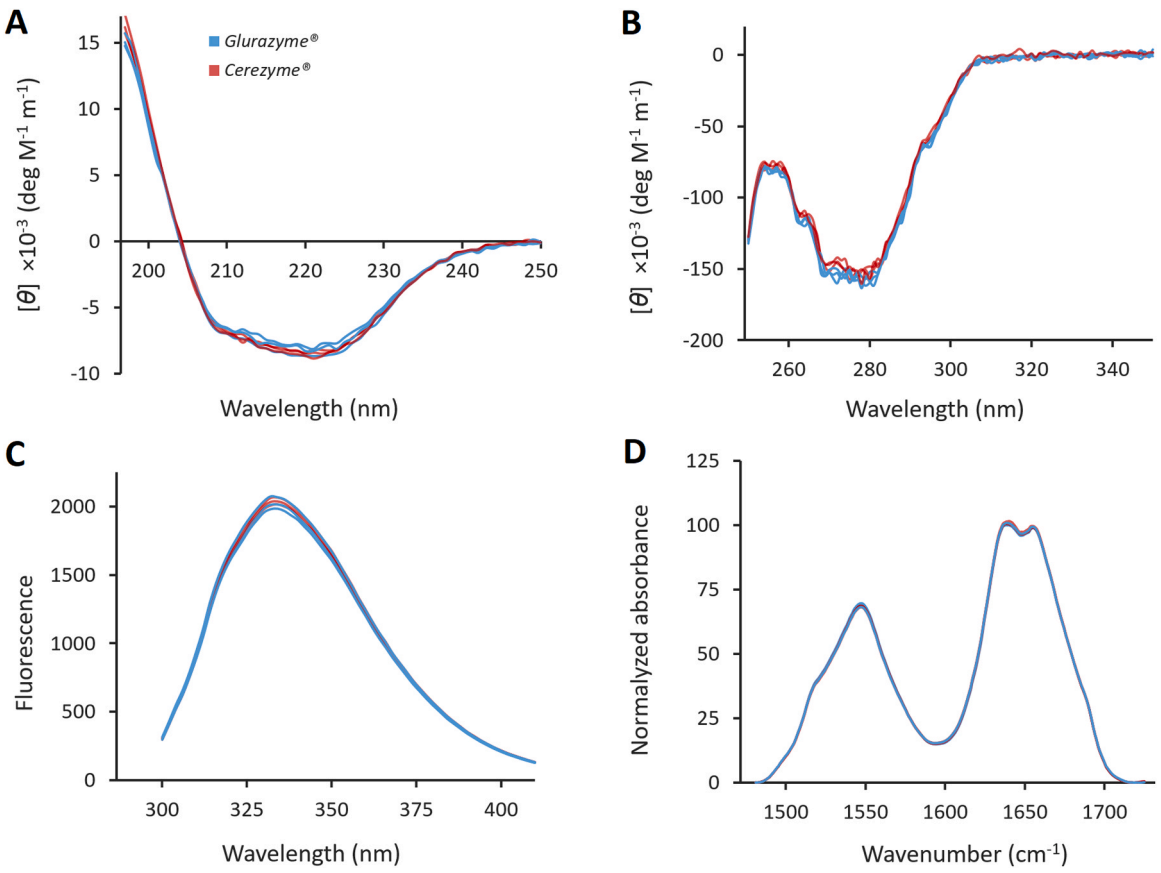

Fig. 3. Superimposition of three Glurazyme® and three Cerezyme® products batches curves: (A) far-UV CD spectra; (B) near-UV CD spectra; (C) FT-IR spectra; and (D) intrinsic fluorescence. Glurazyme® data are shown with blue, while Cerezyme® data are shown with red.

polypeptide theoretical mass is 55,574 Da all the proteoforms found in the study considered to be glycosylated. Among the entire pattern, four most pronounced glycosylated proteoforms has been evaluated (*M3F/M3F/M3F/M3*, *M3FN/M3F/M3F/M3*, *M3FN/M3FN/M3/M3*, *M3FN/M3FN/M3F/M3 +Ox*), that constitutes about 60% of Cerezyme® proteoforms and more than 80% for Glurazyme® samples (Table 1).

3.3. Disulfide bonds

The disulfide bridges network is important for the tertiary structure stabilization, and, consequently, affects protein biological properties. A conserved structure of β-glucocerebrosidase involves the formation of two C4/C16 and C18/C23 covalent bonds while three other cysteines (126, 248, and 342) considered to be spatially isolated [10,21]. The measured total number of thiols per reduced molecule corresponded to 6.5 ± 0.4 (mol/mol) for both Glurazyme® and Cerezyme® products that is consistent with the method variability. A free thiol content estimated by intact imiglucerase samples showed a value of approximately 2.7 (mol/mol) thus confirming a consideration above.

A practical method of disulfide bonds LC-MS/MS mapping allowed to determine the location of disulfide bridges and unpaired protein cysteines simultaneously. A detailed analysis confirmed that both Glurazyme® and Cerezyme® samples contains two disulfides at C4-C16 and C18-C23 positions while three other residues (126, 248, and 342) remains unpaired (Supplementary Fig. 4s).

3.4. Charge variants

Here a slab isoelectric focusing method was used to characterize the content of charged protein isoforms representing a result of additional modifications (deamidation, oxidation, glycosylation, etc.). All

Table 1
Imiglucerase proteoforms identity and distribution.

Proteoform	Exact mass, Da	Measured mass, Da	**Cerezyme®**	**Glurazyme®**
M3F/M3F/M3F/M3	59,583.2	59,583.1	17.9 ± 1.2%	37.7 ± 3.7%
M3FN/M3F/M3F/M3	59,785.7	59,785.9	20.3 ± 0.7%	21.1 ± 2.6%
M3FN/M3FN/M3/M3	59,841.5	59,841.4	13.4 ± 1.5%	9.6 ± 0.4%
M3FN/M3FN/M3F/M3	59,988.2	59,986.1	n.d.	2.2 ± 1.8%
M3FN/M3FN/M3F/M3 + Ox	60,003.2	60,003.2	11.9 ± 1.2%	17.2 ± 0.6%
G0F/M3FN/M3/M3	60,044.6	60,044.0	7.1 ± 0.7%	0.5 ± 0.2%
M3FN/M3FN/M3F/M3F + Ox	60,149.8	60,150.7	4.8 ± 0.1%	4.7 ± 0.3%
M3FN/G0F/M3F/M3	60,191.3	60,191.7	n.d.	1.9 ± 0.4%
M3FN/M3FN/M3FN/M3 + Ox	60,205.7	60,206.1	11.9 ± 0.5%	2.2 ± 0.4%
G0F/G0F/M3/M3	60,247.7	60,246.4	1.9 ± 0.4%	n.d.
M3FN/M3FN/M3FN/M3F + Ox	60,352.3	60,353.2	5.4 ± 0.1%	3.0 ± 0.2%
M3FN/M3FN/G0F/M3	60,393.8	60,393.4	n.d.	1.0 ± 0.1%
G0F/M3FN/M3FN/M3 + Ox	60,408.8	60,408.2	4.4 ± 0.7%	1.1 ± 0.1%
M3FN/M3FN/M3FN/M3FN + Ox	60,554.8	60,554.5	1.8 ± 0.1%	n.d.

Glurazyme® and Cerezyme® samples demonstrate the presence of five separate bands within the range of 6.8–8.2 pI with no unique bands found. Moreover, the statistical analysis of gel densitometry data confirms the high similarity of isoform distribution and proves about 85% of total isoforms to be identical (Fig. 4 and Supplementary Fig. 3s).

3.5. Glycosylation

Imiglucerase molecule contains four asparagine residues (19, 59, 146, and 270) typically occupied by N-glycans [22]. Since oligosaccharides have the potential ability to affect biological, pharmacokinetic, and immunogenic properties the glycosylation pattern is a prerequisite for biosimilarity confirmation. The glycosylation profile has been evaluated by HILIC methodology. An example of fluorescence chromatograms obtained as a result of N-glycans separation is shown in Fig. 5, while the full list of measured monoisotopic masses summarized in supplementary section (Table 3s). Here predominant (more than 70%) modifications represent trimannosylchitobiose structures. Among them *M3, M3F* and *M3FN* glycans are the most abundant. Additionally, high-mannose forms as well as phosphorylated species (*M5*, *M5P*, *M6P*, *M5PN*, and *M6PN*) are noticed, however, in a significantly fewer amount.

To deep understand the glycoforms site distribution we performed a supplementary LC-MS "bottom-up" data inspection. Here all four site-specific glycosylation profiles (i.e. N19, N59, N146, and N270) found to be dominating with *M3, M3F* and *M3FN* variants and looked very similar for both Glurazyme® and Cerezyme® products (Fig. 5). The same is confirmed when the intact mass results are considered (Table 1).

3.6. Related impurities

The used method of size-exclusion HPLC allowed to separate both monomeric and aggregate fractions of imiglucerase. Glurazyme® as well as Cerezyme® elution profiles characterized by a pronounced monomeric form peak with a retention time of about 11.3 min (Supplementary Fig. 5s). At the same chromatogram, aggregates migrate as 9.8 min peak. Both imiglucerase products demonstrate a comparable presence of about 1% of aggregates.

Imiglucerase contains seven conserved cysteines with four of them involving in a disulfide bridges formation. A wrong pairing could bring about a misfold that causes a regular structure distortion. In addition, there can be examples of spontaneous asparagine deamidation, as well as methionine oxidation leading to a similar result [23]. A reverse phase chromatography (RP-HPLC) is a sensitive technique to analyze discrepancies alike.

An example of imiglucerase RP-HPLC chromatograms is shown in Fig. 6. Both products demonstrate the presence of main peak at 12.5 min, while related substances were found within two groups of pre- and post-peaks. For Glurazyme® samples the related substances are on average 0.5% and 2.5% higher as compared to original Cerezyme® pre- and post-peaks, respectively. Taken together, these data suggest a slightly reduced content of the Glurazyme® main peak form.

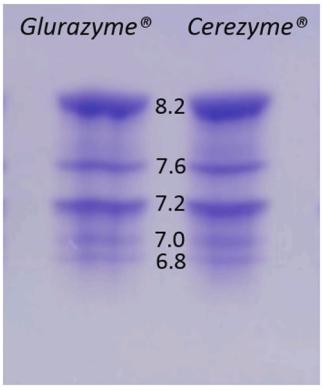

Fig. 4. Electropherogram of imiglucerase charged isoforms. Isoelectric points are shown near corresponding imiglucerase bands.

To assess the criticality of the difference observed, an additional LC-MS study of the pre- and post-peak fractions was performed. Here, molecular masses determined for each peak fraction were used to interpret a possible modifications pattern. As for Cerezyme® accompanying forms the glycans' distribution seemed to be the main reason for these fractions because of the respective mass shift. In a generic Glurazyme® product not only four glyco-sites occupation was a prerequisite for the appearance of concomitant peaks, but multiple oxidized variants were detected consistent with the results of modification profiling (Fig. 2).

3.7. Enzymatic activity

Natural β-glucocerebrosidase is a lysosomal hydrolase involved in catabolism of cell wall components, such as homologous N-acyl-sphingosyl-1-O-β-D glucosides, including glucosylsphingosines without fatty acids. In the present study synthetic substrate analog containing a chromogenic 4-nitrophenyl-β-D-glucopyranoside, as well as natural β-D-glucosylceramide, were employed in accordance with published protocols [24,25].

An example of kinetic curves of two Glurazyme® and Cerezyme® samples is shown in Fig. 7A. Both products performed a hydrolysis with respect to 4-nitrophenyl-β-D-glucopyranoside. Two principal Michaelis-Menten parameters (i.e. K_m and k_{cat}) seemed to be close for imiglucerase preparations under the study. Together with a specific activity level of approximately 40 U/mg, they were reasonably consistent with the published data [25–27]. An alternate study of natural β-D-glucosylceramide hydrolysis was also performed showing the relative activity of Glurazyme® to be within 85–105% interval of Cerezyme® (data not shown).

3.8. MMR binding and internalization

An SPR methodology was employed for the assessment of mannose receptor binding that is prerequisite for successive imiglucerase uptake to macrophages. A dose-dependent equilibrium of protein complexes was monitored under physiological conditions. Dissociation constant values obtained for both Glurazyme® and Cerezyme® appeared to be near 12 nM (Supplementary Table 5s). A desired interaction was further confirmed by direct internalization study to murine peritoneal macrophages expressing sufficient MMR on its plasma membranes [28]. The level of internalized imiglucerase was measured by a more sensitive fluorescence-based assay. As judged by accumulation of 4-methylumbelliferone the relative activity of Glurazyme® samples typically corresponded to 90–110% interval of Cerezyme® (Supplementary Table 6s). In this internalization study the simultaneous addition of mannan to a cell suspension containing imiglucerase resulted in an approximately 2-fold inhibition of product penetration, as assessed by the decrease of 4-methylumbelliferone fluorescence (Fig. 7B). Thus, internalization of Glurazyme® and/or Cerezyme® is significantly reduced in the presence of mannose-containing competitor.

4. Discussion

4.1. Study plan

The evaluation of two drug products analytical comparability based on a direct comparison of quality attributes. A "head-to-head" study was performed with a sufficient number of Cerezyme® batches purchased at the market and commercial (100-liter bioreactor) Glurazyme® batches. By the time of study all the samples had valid expiry dates. Both products were similar by their formulations.

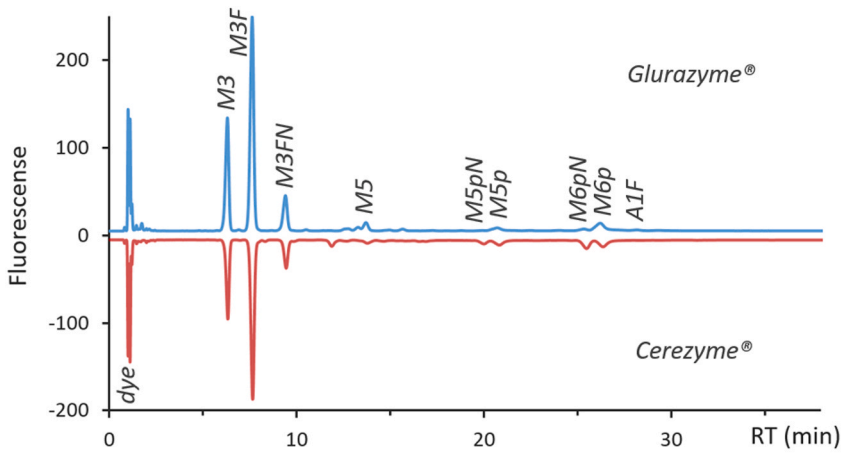

Glycan	Composition	Exact mass, a.m.u.	Measured mass, a.m.u.
M3	Hex3HexNAc2	910.328	910.332
M3F	Hex3HexNAc2Fuc1	1056.386	1056.389
M3FN	Hex3HexNAc3Fuc1	1259.465	1259.471
M5	Hex5HexNAc2	1234.433	1234.438
M5p	Hex5p1HexNAc2	1314.400	1314.406
M5pN	Hex5p1HexNAc3	1517.479	1517.484
M6p	Hex6p1HexNAc2	1476.452	1476.458
M6pN	Hex6p1HexNAc3	1679.532	1679.534
A1F	Hex5HexNAc4Fuc1Neu5Ac1	2077.745	2077.751

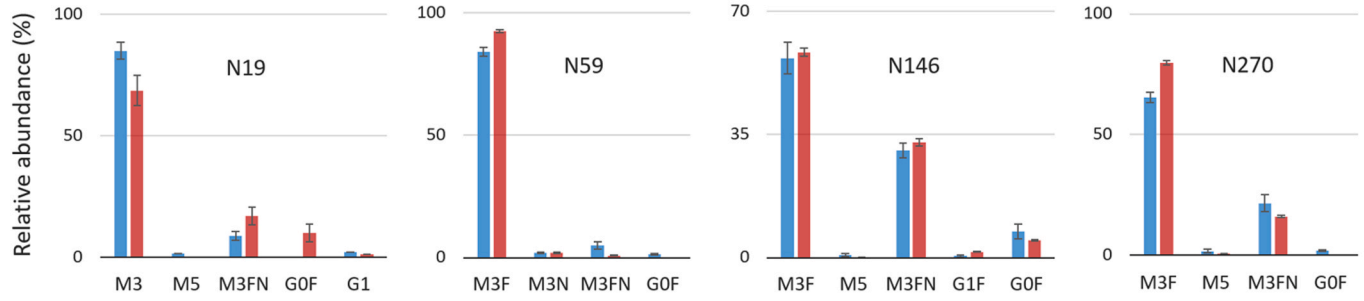

Fig. 5. A mirror plot of chromatograms of imiglucerase product N-glycans with their LC-MS interpretation and distribution among four sites (N19, N59, N146, and N270). Glurazyme® profile is shown with blue, while Cerezyme® profile is shown with red.

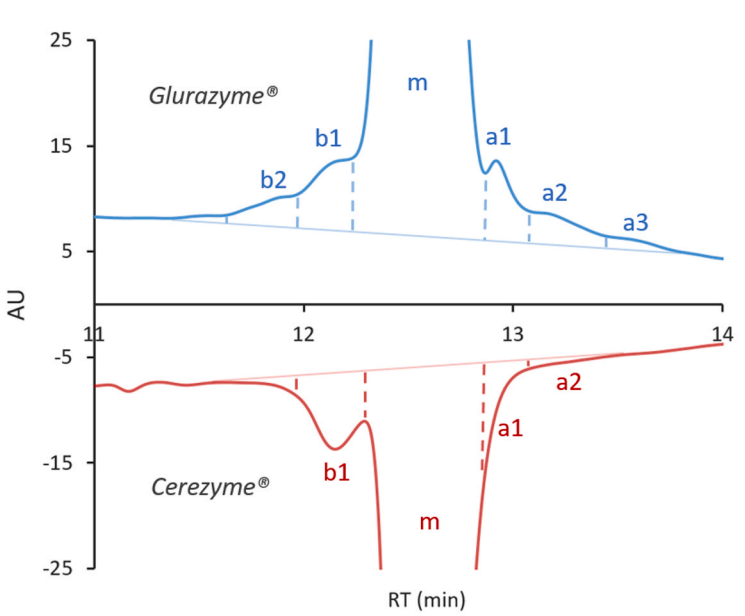

Peak	Exact mass, Da	Measured mass, Da	Proteoform
b2	59599	59600	M3F/M3F/M3F/M3 + *Ox*
b1	59599	59601	M3F/M3F/M3F/M3 + *Ox*
m	59583	59582	M3F/M3F/M3F/M3
a1	60003	60007	M3FN/M3FN/M3F/M3 + *Ox*
a2	60019	60015	M3FN/M3FN/M3F/M3 + 2*Ox*
	59599	59596	M3F/M3F/M3F/M3 + *Ox*
a3	60019	60013	M3FN/M3FN/M3F/M3 + 2*Ox*
	59599	59602	M3F/M3F/M3F/M3 + *Ox*
b1	59696	59714	M3FN/M3N/M3/M3
m	59583	59583	M3F/M3F/M3F/M3
a1	–	–	n.d.
a2	59786	59792	M3FN/M3F/M3F/M3

Fig. 6. A mirror plot of imiglucerase RP-HPLC chromatograms along with LC-MS fraction interpretation. Proteoforms with oxidation are marked with "*Ox*" label.

In accordance with the current regulatory documents of ICH, FDA, and EMA applied for the development of biosimilar products, the plan of analytical comparability assessment had been developed to characterize the structural, physicochemical, and functional similarity [29–32]. This plan was aimed at comparing the properties of active component that can potentially affect the safety and efficacy of the medicinal product. Based on the quality target product profile (QTPP), the permissible ranges of CQA were assumed by measuring the original product Cerezyme® characteristics. Complete characterization was carried out using orthogonal analytical methods when possible.

4.2. *Similarity assessment*

The current study aimed to demonstrate a high physico-chemical similarity of two imiglucerase drug products: Cerezyme® and Glurazyme®. The first one was originally prepared by Genzyme Corp. while

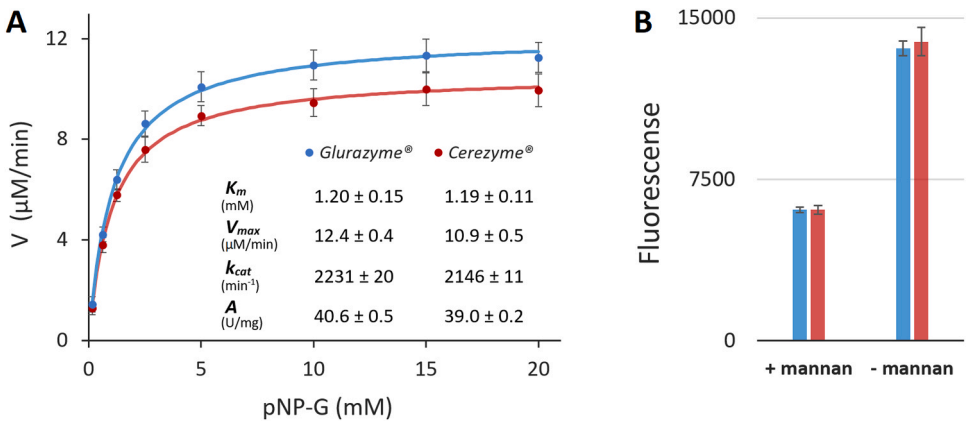

Fig. 7. Evaluation of biological properties: (A) example of Michaelis-Menten kinetics demonstrated by two batches of imiglucerase in relation to the chromogenic substrate pNP-G; (B) inhibiting effect of mannan on imiglucerase internalization by peritoneal macrophages.

the last was developed by Generium LLC. and authorized in several countries for the practical purpose.

Here we demonstrate that both products have an identical primary and high-order structures as judged by direct peptide mapping and spectroscopic investigations. The proteolytic hydrolysates mass-chromatograms of Glurazyme® and Cerezyme® confirm the theoretical amino acid sequence of imiglucerase, and also indicate the differences in the content of methionine oxidized forms as well as deamidated form of glutamine 440 (Fig. 2). Two primary oxidized residues M123 and M450 are located at β-strands transitions linking to disordered areas and, consequently, oriented outside the globule. Such a disposition of methyl sulfide groups promotes a favorable arrangement for oxidizing attack possible during the sample preparation step [33]. Nevertheless, oxidized forms were registered for 11 separate amino acids thus presuming their presence even on the level of intact molecule. A glutamine 440 residue is located in the linker connecting two β-strands and also oriented to the outer space, that increase the availability to potential nucleophilic attack. Together with other less pronounced differences it can be considered non-critical due to the absence of a direct effect on the catalytic activity and/or binding functions of imiglucerase.

Both products demonstrated significant and comparable amounts of succinimide cyclic form in place of 188 asparagine (Fig. 2). Interestingly no respective deamidated species were observed for N188 while N192 demonstrates ammonium loss to some extent. Thus, a major succinimide containing form is supposed to depend on intrinsic properties of a trypsin-generated peptide rather than a real deamidation intermediate [23].

The calculated molecular mass of the amino acid sequence of imiglucerase is 55,574 Da, and the distribution of intact enzyme proteoforms around 60 kDa for both Glurazyme® and Cerezyme® (Table 1) indicates a significant glycosylation in accordance with previous studies [12,34]. 9 of 14 observed proteoforms were reported for both imiglucerase products representing more than 97% of the total content.

Imiglucerase molecule contains five consensus asparagine residues (N-x-S/T) located on the globule surface and available for intracellular glycosylation machinery. Only four of them are actually modified [35]. The results of site-directed mutagenesis confirm the criticality of N19 glycosylation for the catalytic activity of the protein; however, they seem ambiguous with respect to selected substrate or amino acid substitution [36–38]. There are also published data describing a significant oligosaccharide effect on imiglucerase stability in aqueous solution [12]. Taking into account moderate heterogeneity of N-glycans a possible pharmacokinetics effect is under the question.

The imiglucerase mechanism of action implies the endocytosis stage to be mediated by interaction with cellular mannose-binding receptors. It is known that natural β-glucocerebrosidase contains about 20% of high-mannose glycans for this purpose. The other part is unevenly distributed between bi- and triantenna oligosaccharides of complex type. Among 9% of the remaining glycans also contain a terminal mannose residue within uncapped antennas composition [39]. On average, only one fourth of glycosylated sites totality is capable for receptor binding thus reducing an overall efficacy of therapeutic. Internalization is further disturbed by hepatocytes protein absorption via asialoglycoprotein receptor interaction. Artificial glycan remodeling produced by exoglycosidase treatment significantly improves a macrophage binding potency and increases imiglucerase cellular lifetime, thereby influencing on the efficacy [40,41].

Here we confirm imiglucerase glycosylation pattern (Fig. 5) to be consistent with published data [25,42]. A more detailed comparison has revealed some difference between two products. For example, Glurazyme® samples are characterized by increased abundances of trimannosylchitobiose glycans (*M3, M3F, M3FN*) as compared to Cerezyme® that possibly results from incomplete enzymatic remodeling of the originators' biantenna precursors. It becomes more evident via the total mannose glycans content comparison (*M* group in Table 2).

On the other hand, Cerezyme® samples are characterized by increased percentage of high-mannose oligosaccharides containing mannose-6-phosphate residues (*Mp* group in Table 2). Glycans with terminal mannose are believed to play a key role in the efficacy of enzyme replacement therapy for lysosomal storage disorders [43]. Thus, glucocerebrosidase penetration into macrophage cells can be significantly improved, when all four oligosaccharide branches of the molecule contain an external mannose [44]. Both products chromatograms demonstrate peaks of trimannosylchitobiose and high-mannose glycans along with phosphorylated species that can contribute to effective transport via mannose receptor binding. The total content of these modifications is about 90% and within 3–4% differs among the compared products. As a result, one can suggest a high percentage of molecules carrying terminal mannose within four glyco-sites and minimizes the physiological impact of the established difference. The latter is confirmed by intact protein MS data demonstrating glycosylated proteoforms with four trimannosylchitobiose glycans to be the most abundant (Table 1).

Incomplete remodeling is also the reason for sialylated glycoform presence although in a small extent of about 1%. Potentially sialylation affect activity, pharmacokinetics, and immunogenicity of biomolecules, however, under the content observed only the last one can be the key of concern. Fortunately, Chinese Hamster Ovary cells are capable of producing only α-2,3-N-acetylneuraminic acid residues, that excludes any immunogenicity under the scope [45,46].

Incidentally Glurazyme® appear to contain a little more processed oligosaccharides as compared to Cerezyme® judging by the abundance of registered glycoforms containing "unprocessed" G0F species (Table 1). It is the case even with "bottom-up" MS data demonstrating

Table 2
Quality parameters and their assessment.

Parameter	CQA	Risk	Assay	Cerezyme®	Glurazyme®
Primary structure	Primary structure	High	Peptide mapping	profile	profile
Modifications	Deamidation	Moderate	Peptide mapping	4 sites	4 sites
	Oxidation	Moderate	Peptide mapping	11 sites	11 sites
	Succinimide	Low	Peptide mapping	2 sites	2 sites
Higher order structure	Secondary and tertiary	Moderate to high	CD spectroscopy	profile	profile
	Secondary structure	Moderate	FTIR spectroscopy	profile	profile
			UV absorption spectroscopy	profile	profile
	Tertiary structure	Moderate	Intrinsic fluorescence	profile	profile
	Thiols and disulfide bonds	Moderate	Ellman's assay	2.8 ± 0.1 mol/mol	2.7 ± 0.1 mol/mol
			Peptide mapping	C4-C16; C19-C23;	C4-C16; C19-C23;
Molecular mass	Intact protein	Low to moderate	LC-MS	59.6 – 60.6 kDa	59.6 – 60.6 kDa
			SDS-PAGE	64 kDa band	64 kDa band
Charged variants	Charged variants	Moderate to high	Isoelectofocusing	6.8 – 8.2 pI	6.8 – 8.2 pI
Glycosylation	N-glycan profile	Moderate to high	HILIC	(*M*) 73.9 ± 1.3%	(*M*) 85.9 ± 1.4%
				(*Mp*) 16.2 ± 0.5%	(*Mp*) 7.5 ± 0.4%
				(*S*) 0.8 ± 0.1%	(*S*) 0.8 ± 0.1%
			Site-distribution LC-MS	N19; N59; N146; N270;	N19; N59; N146; N270;
Purity/impurities	Aggregates	Moderate to high	Size-exclusion HPLC	0.4 ± 0.1	0.4 ± 0.1
	Hydrophobic proteoforms	Moderate to high	Reversed phase HPLC	6.7 ± 0.6%	9.8 ± 1.0%
Activity	MMR binding	High	SPR	12.2 ± 0.5 nM	12.3 ± 0.6 nM
			Internalization	90 – 115%	92 – 111%
	Enzymatic activity	High	pNP-G cleavage	37.9 ± 2.2 U/mg	37.6 ± 2.3 U/mg
			Glucosylceramide cleavage	78 – 99%	85 – 106%

overall 5% elevation of G0F glycopeptides mainly as a result of N19 glycosylation of Cerezyme®. This reasonably correlates with direct N-glycans measurements and may be associated with a more complete biosimilar remodeling, despite only main glycoforms could be estimated by two mentioned LC-MS methodologies.

A discovered difference of N-glycosylation as well as modified amino acids discrepancies were further subjected for evaluation with isoelectrofocusing and RP-LC approaches. As judged by electropherogram Glurazyme® and Cerezyme® consist of very similar isoform sets with minor distribution discrepancy. A small visual increase for Glurazyme® acidic 7.6 pI isoform is agreed with peptide mapping data showing enlarged glutamine 440 deamidation (Fig. 4). Oxidized forms are mutually estimated by RP-LC methodology and, here, Glurazyme® samples seemed to be a little more pronounced (Fig. 6) that also could contribute to protein “acidification”.

To evaluate risk of activity and pharmacokinetics difference as a result of established modifications we experimentally verified imiglucerase ability for chromogenic and natural substrate cleavage, as well as its binding to mannose receptor and uptake to peritoneal macrophages.

An apparent Michaelis constant (K_m) determined by pNP-G imiglucerase substrate is about 1.2 mM independently on the source of enzyme. Although catalytic rate constant (k_{cat}) values of Glurazyme® and Cerezyme® could potentially reflect the difference between two imiglucerase products we suppose it to be the consequence of two particular samples shelf-lives. The last one looks to be the case since calculated over the number of batches activities correspond to 37.6 ± 2.3 and 37.9 ± 2.2 U/mg for Glurazyme® and Cerezyme® respectively (Table 2). The other very similar activity attributes of two products were obtained in the study with natural β-D-glucosylceramide substrate. Glurazyme® relative activity was about 85–105% of that of Cerezyme® evidencing for the identical β-D-glucosylceramide degradation (data not shown).

As the main function of lysosomes is cleavage of internalized material by specific hydrolases, that’s why associated organelles represent a system of compartments interacting with environment through endocytosis, phagocytosis, and exocytosis. Lysosomal enzymes are typically synthesized and matured by acquiring carbohydrate recognition markers, necessary for their transportation via specific receptors [43]. Since this mechanism is fundamental for imiglucerase an SPR method was used to monitor dose-dependent equilibrium of protein-mannose-receptor complexes under physiological conditions. As measured apparent dissociation constants correspond to 12.1 ± 0.6 nM and 12.3 ± 0.5 nM for MMR complexes of Glurazyme® and Cerezyme®, respectively thereby meeting the expectations. When assessing the specificity of imiglucerase product penetration to peritoneal macrophages, the simultaneous addition of mannan led to a 2-fold inhibition of 4-methylumbelliferyl-β-D-glucopyranoside hydrolysis for both Glurazyme® and Cerezyme® (Fig. 7B). An equivalence testing over the number of imiglucerase batches proves the identical mannose-receptor binding affinities as well as macrophage uptake (Supplementary Tables 5s and 6 s). In other words, internalization of the generic product Glurazyme®, as well as the original Cerezyme® occurs similar via receptor-mediated endocytosis through the binding of external mannose residues.

5. Conclusion

With combination of a number of analytical techniques a deep physicochemical and biological characterization of Glurazyme® biosimilar versus the reference originator product Cerezyme® has been performed. The difference observed for imiglucerase products in the content and distribution of N-glycans, as well as oxidized and deamidated amino acid residues supposed to be insignificant regarding the effect on pharmacokinetics, immunogenicity, and catalytic properties. The other estimated CQAs so as primary and high-order structures, free sulfhydryl groups, aggregated forms, mannose-receptor affinity and ability to hydrolyze either synthetic or natural substrates have been shown to be identical for both imiglucerase products.

All the collected data confirms the high comparability of functional and physicochemical properties (Table 2). Based on the information obtained, we can confidently state that generic product Glurazyme® has a high degree of comparability with respect to the reference originator product Cerezyme® that has been successfully verified within clinical practice [47,48].

CRediT authorship contribution statement

Degterev Maksim: Formal analysis, Investigation, Validation. **Lyagoskin Ivan:** Data curation, Formal analysis, Investigation, Validation. **Neronova Maria:** Investigation, Validation. **Taran Serge:** Formal analysis, Investigation, Methodology, Writing – review & editing. **Smolov Maksim:** Conceptualization, Formal analysis, Investigation, Visualization, Writing – original draft, Writing – review & editing, Data curation. **Shukurov Rakhim:** Project administration, Supervision.

Declaration of Competing Interest

The authors declare that they have no known competing financial interests or personal relationships that could have appeared to influence the work reported in this paper.

Acknowledgements

We thank Igor Fabrichny and Mikhail Razumikhin (JSC "Generium") for providing an effective imiglucerase remodulation and purification protocol as well as helpful advice in analytical study design.

Appendix A. Supporting information

Supplementary data associated with this article can be found in the online version at doi:10.1016/j.jpbao.2023.100024.

References

[1] G.A. Grabowski, G.A. Petsko, E.N. Kolodny, Gaucher Disease, in: D.L. Valle, S. Antonarakis, A. Ballabio, A.L. Beaudet, G.A. Mitchell (Eds.), The online metabolic and molecular bases of inherited disease, McGraw Hill, 2019, https://doi.org/10.1036/ommbid.419.
[2] A.H. Futerman, Cellular pathology in Gaucher disease (Florida), in: A.H. Futerman, A. Zimran (Eds.), Gaucher Disease, Vol 1, CRC Press, Boca Raton, 2006, pp. 97–108, https://doi.org/10.1201/9781420005509 (Florida).
[3] P.J. Meikle, J.J. Hopwood, A.E. Clague, W.F. Carey, Prevalence of lysosomal storage disorders, JAMA 281 (1999) 249–254, https://doi.org/10.1001/jama.281.3.249.
[4] P.J. Meikle, M. Fuller, J.J. Hopwood, Epidemiology and screening policy (Florida), in: A.H. Futerman, A. Zimran (Eds.), Gaucher Disease, Vol 1, CRC Press, Boca Raton, 2006, pp. 321–340, https://doi.org/10.1201/9781420005509.ch17 (Florida).
[5] S.M. Kulikov, R.V. Ponomarev, K.A. Lukina, E.P. Sysoeva, E.A. Lukina, The Russian National Gaucher registry, Vol 2(S1), HemaSphere, 2018.
[6] G. Drelichman, G. Castañeda-Hernández, A.M. Cem, M. Dragosky, R. Garcia, H. Lee, et al., The road to biosimilars in rare diseases – ongoing lessons from Gaucher disease, Am. J. Hematol. 95 (2020) 233–237, https://doi.org/10.1002/ajh.25701.
[7] J. Rasmussen, G. Barsomian, M. Bergh, Enzymatically active recombinant glucocerebrosidase, US patent 5 236 838, 1993.
[8] B. Friedman, M. Hayes, Enhanced in vivo uptake of glucocerebrosidase, US patent 5 549 892, 1996.
[9] B. Henrissat, A. Bairoch, New families in the classification of glycosylhydrolases based on amino acid sequence similarities, Biochem. J. 293 (1993) 781–788, https://doi.org/10.1042/bj2930781.
[10] H. Dvir, M. Harel, A.A. McCarthy, L. Toker, I. Silman, A.A. Futerman, J.L. Sussman, X-Ray structure of human acid-b-glucosidase, the defective enzyme in Gaucher disease, EMBO Rep. 4 (2003) 704–709, https://doi.org/10.1038/sj.embor.embor873.
[11] R.J. Tamargo, A. Velayati, E. Goldin, E. Sidransky, The role of saposin C in Gaucher disease, Mol. Genet. Metab. 106 (2012) 257–263, https://doi.org/10.1016/j.ymgme.2012.04.024.
[12] Y. Kacher, B. Brumshtein, S. Boldin-Adamsky, L. Toker, A. Shainskaya, I. Silman, et al., Acid beta-glucosidase: insights from structural analysis and relevance to Gaucher disease therapy, Biol. Chem. 389 (2008) 1361–1369, https://doi.org/10.1515/BC.2008.163.
[13] International Conference on Harmonization (ICH), Q2(R1): Validation of Analytical Procedures: Text and Methodology, 2005. ⟨https://www.ich.org⟩.
[14] Mini-PROTEAN® II Electrophoresis Cell Instruction Manual, M1652940 Revision B, Bio-Rad.
[15] P.W. Riddles, R.L. Blakeley, B. Zerner, Ellman's reagent: 5,5′-dithiobis(2-nitrobenzoic acid) – a reexamination, Anal. Biochem. 94 (1979) 75–81, https://doi.org/10.1016/0003-2697(79)90792-9.
[16] J.M. Walker, Isoelectric focusing (IEF) of proteins in thin-layer polyacrylamide gels, in: R.J. Slater (Ed.), Experiments in molecular biology. Springer Protocols Handbooks, Humana Press, Totowa, New Jersey, 1986, pp. 161–169, https://doi.org/10.1007/978-1-60327-405-0_16.
[17] M. Kimzey, Z. Szabo, V. Sharma, A. Gyenes, S. Tep, A. Taylor, et al., Development of an Instant glycan labeling dye for high throughput analysis by mass spectrometry, ProZyme (2015) 4.
[18] Biacore 8K System Handbook, Revision 29165960 AB, 2016, GE Healthcare.
[19] G.H. Beaven, E.R. Holiday, Ultraviolet absorption spectra of proteins and amino acids, in: M.L. Anson, K. Bailey, J.T. Edsall (Eds.), Advances in protein chemistry, Vol. 7, Academic Press, 1952, pp. 319–386, https://doi.org/10.1016/S0065-3233(08)60022-4.
[20] P.R. Callis, B.K. Burgess, Tryptophan fluorescence shifts in proteins from hybrid simulations: an electrostatic approach, J. Phys. Chem. B 101 (1997) 9429–9432, https://doi.org/10.1021/jp972436f.
[21] R. Moharram, D. Maynard, E.S. Wang, A. Makusky, G.J. Murray, B.M. Martin, Reexamination of the cysteine residues in glucocerebrosidase, FEBS Lett. 580 (2006) 3391–3394, https://doi.org/10.1016/j.febslet.2006.04.096.
[22] B. Brumshtein, M.R. Wormald, I. Silman, A.H. Futerman, J.L. Sussman, Structural comparison of differently glycosylated forms of acid-b-glucosidase, the defective enzyme in Gaucher disease, Acta Crystallogr. D. Biol. Crystallogr. 62 (2006) 1458–1465, https://doi.org/10.1107/S0907444906038303.
[23] R.C. Stephenson, S. Clarke, Succinimide formation from aspartyl and asparaginyl peptides as a model for the spontaneous degradation of proteins, J. Biol. Chem. 264 (11) (1989) 6164–6170, https://doi.org/10.1016/S0021-9258(18)83327-0.
[24] O. Motabar, E. Goldin, W. Leister, K. Liu, N. Southall, W. Huang, et al., A high throughput glucocerebrosidase assay using the natural substrate glucosylceramide, Anal. Bioanal. Chem. 402 (2012) 731–739, https://doi.org/10.1007/s00216-011-5496-z.
[25] Y. Tekoah, S. Tzaban, T. Kizhner, M. Hainrichson, A. Gantman, M. Golembo, et al., Glycosylation and functionality of recombinant β-glucocerebrosidase from various production systems, Biosci. Rep. 33, e00071. https://doi.org/10.1042/BSR20130081.
[26] S.M. Van Patten, H. Hughes, M.R. Huff, P.A. Piepenhagen, J. Waire, H. Qiu, et al., Effect of mannose chain length on targeting of glucocerebrosidase for enzyme replacement therapy of Gaucher disease, Glycobiology 17 (2007) 467–478, https://doi.org/10.1093/glycob/cwm008.
[27] S. Pokorna, O. Khersonsky, R. Lipsh-Sokolik, A. Goldenzweig, R. Nielsen, Y. Ashani, et al., Design of a stable human acid-β-glucosidase: towards improved Gaucher disease therapy and mutation classification, FEBS J. 290 (2013) 3383–3399, https://doi.org/10.1111/febs.16758.
[28] H.J.P. van der Zande, D. Nitsche, L. Schlautmann, B. Guigas, S. Burgdorf, The mannose receptor: from endocytic receptor and biomarker to regulator of (meta) inflammation, Front. Immunol. 12 (2021), 765034, https://doi.org/10.3389/fimmu.2021.765034.
[29] WHO Guidelines on evaluation of similar biotherapeutic products (SBPs). In: WHO expert committee on biological standardization: 67th report. Geneva: World Health Organization; 2017: Annex 2 (Technical report series No. 1004) p. 616.
[30] U.S. Department of health and human services, food and drug administration center for drug evaluation and research, center for biologics evaluation and research. Development of therapeutic protein biosimilars: comparative analytical assessment and other quality-related considerations. Draft guidance for industry, 2019, p. 28.
[31] U.S. Department of health and human services, food and drug administration, center for drug evaluation and research, center for biologics evaluation and research. Quality considerations in demonstrating biosimilarity of a therapeutic protein product to a reference product. Guidance for industry, 2015, p. 19.
[32] European Medicines Agency. Guideline on similar biological medicinal products containing biotechnology-derived proteins as active substance: quality issues (revision 1), 2014, p. 9.
[33] T. Mouchahoir, J.E. Schiel, Development of an LC-MS/MS peptide mapping protocol for the NISTmAb, Anal. Bioanal. Chem. 410 (2018) 2111–2126, https://doi.org/10.1007/s00216-018-0848-6.

[34] F.Y. Choy, M. Woo, Purification and the effect of peptide N-glycosidase F on lysosomal membrane-bound glucocerebrosidase from human cultured fibroblasts, Biochem. Cell. Biol. 69 (1991) 551–556, https://doi.org/10.1139/o91-081.
[35] A.H. Erickson, E.I. Ginns, J.A. Barranger, Biosynthesis of the lysosomal enzyme glucocerebrosidase, J. Biol. Chem. 260 (1985) 14319–14324, https://doi.org/10.1016/S0021-9258(17)38720-3.
[36] M.E. Grace, G.A. Grabowski, Human acid b-glucosidase: glycosylation is required for catalytic activity, Biochem. Biophys. Res. Commun. 168 (1990) 771–777, https://doi.org/10.1016/0006-291x(90)92388-g.
[37] M.E. Grace, P.N. Graves, F.I. Smith, G.A. Grabowski, Analysis of catalytic activity and inhibitor binding of human acid b-glucosidase by site directed mutagenesis, J. Biol. Chem. 265 (1990) 6827–6835, https://doi.org/10.1016/S0021-9258(19)39223-3.
[38] A. Berg-Fussman, M.E. Grace, Y. Ioannou, G.A. Grabowski, Human acid b-glucosidase. N-glycosylation site occupancy and the effect of glycosylation on enzymatic activity, J. Biol. Chem. 268 14861–14866. https://doi.org/10.1016/S0021–9258(18)82412–7.
[39] S. Takasaki, G.J. Murray, F.S. Furbish, R.O. Brady, J.A. Barranger, A. Kobata, Structure of the N-asparagine-linked oligosaccharide units of human placental beta-glucocerebrosidase, J. Biol. Chem. 259 (1984) 10112–10117, https://doi.org/10.1016/S0021-9258(18)90936-1.
[40] N.W. Barton, R.O. Brady, J.M. Dambrosia, A.M. Di Bisceglie, S.H. Doppelt, S. C. Hill, et al., Replacement therapy for inherited enzyme deficiency – macrophage-targeted glucocerebrosidase for Gaucher's disease, N. Engl. J. Med. 324 (1991) 1464–1470, https://doi.org/10.1056/NEJM199105233242104.
[41] N.W. Barton, F.S. Furbish, G.J. Murray, M. Garfield, R.O. Brady, Therapeutic response to intravenous infusions of glucocerebrosidase in a patient with Gaucher disease, Proc. Natl. Acad. Sci. Usa. 87 (1990) 1913–1916, https://doi.org/10.1073/pnas.87.5.1913.
[42] B. Brumshtein, P. Salinas, B. Peterson, V. Chan, I. Silman, J.L. Sussman, et al., Characterization of gene-activated human acid-beta-glucosidase: crystal structure, glycan composition, and internalization into macrophages, Glycobiology 20 (2010) 24–32, https://doi.org/10.1093/glycob/cwp138.
[43] V. Shepherd, P. Schlesinger, P. Stahl, Receptors for lysosomal enzymes and glycoproteins, Curr. Top. Membr. Transp. 18 (1983) 317–338, https://doi.org/10.1016/S0070-2161(08)60535-3.
[44] F.S. Furbish, C.J. Steer, N.L. Krett, J.A. Barranger, Uptake and distribution of placental glucocerebrosidase in rat hepatic cells and effects of sequential deglycosylation, Biochim. Biophys. Acta 673 (1981) 425–434, https://doi.org/10.1016/0304-4165(81)90474-8.
[45] D. Ghaderi, R.E. Taylor, V. Padler-Karavani, S. Diaz, A. Varki, Implications of the presence of N-glycolylneuraminic acid in recombinant therapeutic glycoproteins, Nat. Biotech. 28 (2010) 863–867, https://doi.org/10.1038/nbt.1651.
[46] M.N. Fukuda, H. Sasaki, L. Lopez, M. Fukuda, Survival of recombinant erythropoietin in the circulation: the role of carbohydrates, Blood 73 (1989) 84–89, https://doi.org/10.1182/blood.V73.1.84.84.
[47] E.P. Sysoeva, R.V. Ponomarev, K.A. Lukina, R.B. Chavynchak, S.B. Korotkova, M. V. Zhilyaeva, et al., Evaluation of the efficacy and safety of the biosimilar drug Glurazyme (imiglucerase) in patients with Gaucher disease type 1, Russ. J. Hematol. Transf. 65 (2020) 8–23, https://doi.org/10.35754/0234-5730-2020-65-1-8-23.
[48] S.B. Fitilev, A.V. Vozzhaev, I.I. Shkrebneva, D.A. Kudlay, E.V. Gapchenko, O. A. Markova, et al., Results of a phase I open randomized comparative crossover clinical trial to assess the safety and pharmacokinetics of Glurazyme® (imiglucerase) in comparison with the reference product in healthy volunteers, Oncohematology 14 (2019) 73–83, https://doi.org/10.17650/1818-8346-2019-14-4-73-83.